International Journal of Information, Control and Computer Sciences
ISSN: 2517-9942
Vol:9, No:5, 2015

Solar Radiation Time Series Prediction

Cameron Hamilton, Walter Potter, Gerrit Hoogenboom, Ronald McClendon, Will Hobbs

***Abstract*—**A model was constructed to predict the amount of solar radiation that will make contact with the surface of the earth in a given location an hour into the future. This project was supported by the Southern Company to determine at what specific times during a given day of the year solar panels could be relied upon to produce energy in sufficient quantities. Due to their ability as universal function approximators, an artificial neural network was used to estimate the nonlinear pattern of solar radiation, which utilized measurements of weather conditions collected at the Griffin, Georgia weather station as inputs. A number of network configurations and training strategies were utilized, though a multilayer perceptron with a variety of hidden nodes trained with the resilient propagation algorithm consistently yielded the most accurate predictions. In addition, a modeled direct normal irradiance field and adjacent weather station data were used to bolster prediction accuracy. In later trials, the solar radiation field was preprocessed with a discrete wavelet transform with the aim of removing noise from the measurements. The current model provides predictions of solar radiation with a mean square error of 0.0042, though ongoing efforts are being made to further improve the model's accuracy.

***Keywords*—**Artificial Neural Networks, Resilient Propagation, Solar Radiation, Time Series Forecasting.

I. Introduction

THE ability to predict how a quantity will change in the future is a valuable ability to have, as doing so can enable the interested parties to plan accordingly. For instance, accurately predicting how stock prices will evolve can help investors to reduce risk in their investments and maximize their payoffs. Likewise, predicting commodity prices can help businesses know when to purchase certain items in bulk and when to avoid purchases. With respect to safety, the prediction of natural disasters, such as earthquakes [1] can alert people to impending danger such that they can evacuate potentially critical areas before the disaster occurs. These examples demonstrate how predictive models can be used to improve quality of life, but they are only a small sample of the ways in which predictive models can be utilized.

Solar radiation forecasting is a problem within time series prediction that has received considerable attention, as such predictions can inform the expected yield from crops in a given year or the amount of energy that can be produced from a solar panel [2]-[3]. One common model for solar radiation prediction is an artificial neural network (for examples, see [4]-[6]), as these networks serve as universal function approximators [7].Although other models and techniques exist for time series prediction such as support vector machines (SVM), hidden Markov models (HMM), dynamic Bayesian networks (DBN), and autoregressive integrated moving average (ARIMA) models, artificial neural networks (ANNs) have the advantage of accepting multiple data fields as input, rather than being limited to univariate input. Furthermore, ANNs are highly customizable in how the network can be configured (e.g. how many hidden layers/nodes, feedforward vs. recurrent, etc.) and can thus be tailored to a specific problem more readily. As solar radiation is influenced by a number of environmental and atmospheric conditions, an ANN was selected as the most appropriate model for the current study.

Direct normal irradiance (DNI) is the amount of solar radiation that will make contact with a given area under cloudless sky conditions [8]. As the actual amount of solar radiation that is measured locally has been subjected to environmental factors (e.g. cloud coverage, atmospheric gases) before it is measured, DNI can serve as a point of comparison when analyzing solar radiation data. Thus, DNI appears to be a useful field to train an artificial neural network with for the sake of predicting the actual amount of solar radiation, as the two fields should be strongly correlated. The present model utilizes a modeled DNI field in conjunction with measured solar radiation, in order to predict solar radiation one hour into the future.

Discrete Wavelet Transform (DWT) is a technique commonly used for noise reduction in signal processing and data compression [9]. The current study treats the solar radiation field as a signal and decomposes the signal into an orthogonal set of wavelets, then reconstructs the signal with the noise removed [10]. Thus, preprocessing the solar radiation field with DWT was hypothesized to be an effective technique for improving the model's prediction accuracy.

In the present study, a model was constructed to predict the amount of solar radiation that will make contact with the surface of the earth in a given location an hour into the future. This study was supported by the Southern Company with the idea that the model could be used to determine at what specific times during a given day of the year solar panels could be relied upon to produce energy in sufficient quantities. An artificial neural network was used to approximate the nonlinear pattern of solar radiation, which utilized measurements of weather conditions collected at the Griffin, Georgia weather station as inputs. As shown in Figs. 1 and 2, the overall trend of increasing solar radiation through the

C. Hamilton is with the Institute of Artificial Intelligence, University of Georgia, Athens, GA 30606 USA (e-mail: crh37207@uga.edu).
W. Potter is with the Institute of Artificial Intelligence, the College of Engineering, and the Department of Computer Science, University of Georgia, Athens, GA 30606 USA (e-mail: potter@uga.edu).
G. Hoogenboom was with the Institute of Artificial Intelligence, and the College of Engineering, University of Georgia, Athens, GA 30606 USA. He is now with AgWeatherNet, Washington State University, Prosser, WA USA
R. McClendon is with the Institute of Artificial Intelligence, and the College of Engineering, University of Georgia, Athens, GA 30606 USA.
W. Hobbs is with Renewable Energy Research Department, Southern Company, Birmingham, AL 35061 USA.

spring and summer and the decrease starting in the fall is present in the solar radiation data from year to year. However, the amount of solar radiation occurring on a given day at a given time can vary drastically between years, which prevent linear approximation techniques from yielding accurate predictions. A number of network configurations and training strategies were utilized, though a multilayer perceptron with a variety of hidden nodes trained with the resilient propagation algorithm consistently yielded the most accurate predictions. In addition, a modeled DNI field and adjacent weather station data were used to bolster prediction accuracy. In later trials, the solar radiation field was preprocessed with a discrete wavelet transform with the aim of removing noise from the measurements. In sum, the current model provides predictions of solar radiation with a mean square error of 0.0042, though ongoing efforts are being made to further improve the model's accuracy.

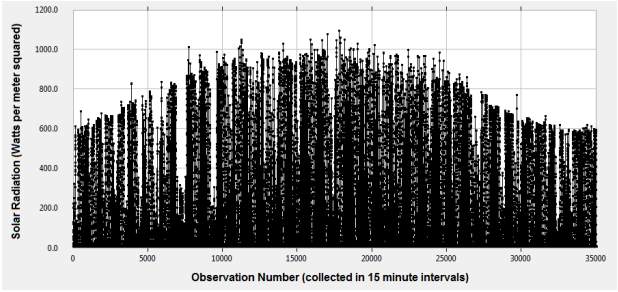

Fig. 1 Solar radiation data collected in 15 minute intervals from the Griffin, Georgia weather station in 2003

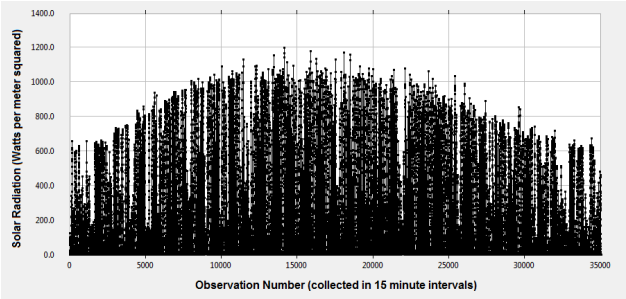

Fig. 2 Solar radiation data collected in 15 minute intervals from the Griffin, Georgia weather station in 2013

II. Materials

Data from the Griffin, Georgia weather station from 2003-2013 were used to build the observations for the input layer to the neural network. Observations were collected at 15 minute intervals over the duration of each year for a total of 35040 observations per year. Forty-three data fields were observed, though only a subset of these fields was used for solar radiation prediction: year, day of year, time of day, air temperature (°C), humidity (%), dew point (°C), vapor pressure (kPa), barometric pressure (kPa), wind speed (m/s), solar radiation (W/m2), total solar radiation (KJ/m2), photosynthetically active radiation (umole/m2s), and rainfall (mm). In later models, measurements of solar radiation from the Williamson, GA weather station - the weather station nearest to the Griffin station - were incorporated as input into the neural network, as data field measurements from nearby adjacent weather stations have been shown to improve performance of solar radiation predictions [11].

In order to further improve prediction accuracy, values for direct normal irradiance (DNI) were modelled for each time step. In addition to the observed fields at the Griffin station, observations of aerosol optical depth, water vapor, and Angstrom's coefficient were taken from AERONET (http://aeronet.gsfc.nasa.gov) at the Georgia Tech site, and used to calculate DNI across the different DNI models implemented. Five separate models were used to calculate the DNI field: WGEN [12], Hoogenboom's [13], Yang's model [14], Iqbal's model [15], and ESRA2 [16], [17]. These models were selected as they have been shown to be some of the most accurate models for modeling DNI [8], [18].

III. Methods

The fields used for prediction of future solar radiation values were first extracted from the raw measurement files from the Griffin station. For each value of the extracted fields at time step t (with the exception of year, day, and time), values from the four previous time steps (t-1, t-2, t-3, t-4) were added to the observation file that would serve as input into the input layer of the neural network. This is known as the sliding window technique and has been shown to significantly increase the accuracy of time series predictions with neural networks [19]. In addition, delta values were calculated for each data field instance by subtracting the previous value from the current value, and were added to the observation file as well.

Modeled values of direct normal irradiance (DNI) were then calculated and added to the observation file for each time step, in addition to their corresponding previous time step and delta values. Although each model varied in the measured and modeled fields used for calculation of DNI, there were some common fields utilized in most or all of the models. The most utilized fields in calculating DNI were solar declination angle (1), hour angle (2), solar elevation angle (3), zenith angle (4), and relative air mass (5), as shown in (1)-(5):

$$DA = \sin^{-1}(\sin 23.35 * \sin(\frac{360}{365} * (day - 81))) \quad (1)$$

$$HA = 15 * (lst - 12), where\ lst\ is\ local\ solar\ time \quad (2)$$

$$EA = 90 - Latitude + DA \quad (3)$$

$$ZA = 90 - EA \quad (4)$$

$$m = \frac{1}{\cos ZA} \quad (5)$$

After the extracted data fields, the modeled DNI values, and (in later models) the solar radiation values from the Williamson station were added to the observation file, each value within the file was scaled within a range of 0 to 1 or -1

to 1 depending on experiment, in proportion to the minimum and maximum values within their respective fields. In the most recent prediction models, the scaled values for the solar radiation field were extracted from the observation file, processed through a discrete wavelet transform (DWT), and inserted back into the observation file. The JWave Java library was used to perform the DWTs. Haars, Coiflet, Daubechie, and Legendre wavelet transforms were performed on the solar radiation field in separate trials in 1-D, 2-D, and 3-D. Once the solar radiation field was transformed and replaced within the observation file, the scaled fields were input into the neural network that was implemented using the Encog Java library.

The Encog Machine Learning Framework available from Heaton Research (Encog) was the primary implementation platform for this research project. It is an extremely robust package for machine learning, providing an extensive library of neural network techniques as well as a multitude of variants and features for each, from adaptive resonance theory networks to Hopfield networks, and backpropagation to evolution-based training. Custom development was done using the Java programming language. Integrating the solar radiation prediction problem into the Encog framework turned out to be somewhat more challenging than the Encog documentation indicates. However, once the Encog environment was setup, changing any of the neural network features was reasonably straight forward. For example, changing from resilient propagation to backpropagation or vice versa was only a matter to changing a few lines of Java code in our custom experiment program. Likewise, making changes to the network architecture such as number of hidden layers and/or number of hidden nodes was a straight forward change, as was invoking cross-validation; all features tweaked to improve prediction performance. In addition to the Encog package, we also investigated using several other packages, namely Neuroshell, Neuroph, and Weka. In a nutshell, we found that Encog was indeed suited our purposes better than these other packages in terms of ease of use, depth of features, and compatibility with the solar radiation project (e.g., handling very large observations files).

The primary bottleneck regarding the use of Encog was providing the proper observations in the proper manner for Encog to use. The process of preparing observations started with the raw data records which were manipulated using a custom routine that created an initial observations file with the specific raw data fields and any supplementary fields needed for the current experiment. The observations file was then converted to a binary observations file where (1) all field values were scaled according to the field minimum and maximum values using a custom module (a common and recommended practice) and then (2) optimized for fast processing using an Encog module. This binary observations file was used by Encog to execute the experimental neural network configuration. With respect to managing an observations file, Encog has special features for allowing the user to either fully read in and store the file in main memory, or process the observations in a batch fashion (one record at a time, and making multiple passes through the file according to what the neural network needs). A weakness of several other popular machine learning packages is the way they handle observations files, and, in particular, the limitations they place on the number of observations they were capable of managing.

One feature of Encog that meshed well with our project approach was the ability to develop custom experiment code that invoked the main features of Encog. This is due to the fact that Encog is itself a large Java program platform. Our approach involved four main components. The first was a Java program that built the observations file using the raw weather data file as input. The next module was a program that converted the observations file into the Encog binary file format using various Encog binary file creation modules. The main model development program came next. It actually performed the model development, that is, created and trained the neural network using the binary observations file as input and our user defined network parameters identified with Encog module features that we set for each specific experiment. Finally, we developed a program (again incorporating Encog module features) that represented the operational version of the solar radiation prediction neural network. It used the trained neural network from the model development process and was intended to make actual, real-time solar radiation predictions. However, model development is the focus of this paper.

During model development, a number of network configurations and training regimes were tested, in addition to varying combinations of input fields, in an effort to determine the setup that would yield the most accurate solar radiation predictions. Trials began with a standard multi-layer perceptron (MLP) network configuration with 29 input nodes, 57 hidden nodes and 1 output node that provided the prediction of solar radiation one hour into the future. In subsequent trials, the number of hidden nodes was adjusted within a range of 17-257 nodes. The initial trials used air temperature, humidity, dew point, barometric pressure, wind speed, solar radiation, total solar radiation, photosynthetically active radiation, and rainfall as the input fields into the neural network. In later trials, various combinations of these fields were used. Furthermore, the backpropagation algorithm was used to train the neural network in the initial trials, but was then replaced with the resilient propagation algorithm (iRPROP+) [20], [21] which consistently yielded more accurate predictions across network configurations.

As a recurrent neural network is not only dependent on the current input as a MLP is, but is also dependent on previous inputs stored in the context layer [22], [23], it was hypothesized that an Elman network would yield more accurate results than a MLP network. An Elman network with 57 hidden nodes was configured and trained with a hybrid strategy of resilient propagation and simulated annealing (SA). The following trials replaced simulated annealing with particle swarm optimization (PSO) for the training strategy. An incremental pruning regime was then implemented which tested the mean squared error (MSE) for networks with successively larger hidden layers until the addition of hidden nodes no longer improved the MSE returned. PSO and SA

were then used independently to train the Elman network after a hidden layer configuration was determined through incremental pruning.

A series of radial basis function networks (RBFNs) were then implemented for solar radiation prediction. The initial RBFN was configured with 49 hidden nodes and a Gaussian radial basis function. In the trials that followed, the centers and widths of the radial basis functions were randomized. Subsequent networks used a Mexican Hat radial basis function and a hidden layer with hidden nodes within the range of 81-196. Singular value decomposition (SVD) was then used to train a RBFN with 196 hidden nodes.

The network type was then switched to a support vector machine with the same 29 input nodes. After the SVM trials were carried out, the model was switched back to a MLP neural network with 157-207 hidden nodes and trained with the resilient propagation algorithm. Within these trials, modeled DNI values and adjacent weather station data were included, in addition to solar radiation preprocessing with DWT.

IV. Results

A MLP network with 157 hidden nodes was consistently shown to be the network configuration that yielded the most accurate solar radiation predictions. The most accurate model achieved an MSE of 0.0042 after 4000 epochs using air temperature, humidity, solar radiation (SR), total solar radiation (TSR), photosynthetically active radiation (PAR) and rainfall as the input fields. See Table III for samples of configurations used in the experiments. The network was able to attain the same accuracy after the TSR and PAR fields were removed. Furthermore, the same network setup with air temperature, humidity, SR and DNI (WGEN model) also achieved an MSE of 0.0042. These results were obtained without preprocessing the SR data through DWT or the adjacent weather station data. The greatest accuracy of the remaining network configurations, input field combinations, and training regimes implemented are summarized in Tables I and II.

TABLE I
Final MSE without DNI, DWT or Adjacent Stations

	# of Hidden Nodes	Training Regime	Epochs	MSE	Notes
MLP	57	RPROP/SA	14	0.008	Greedy
Elman	57	RPROP/SA	250	0.007	Ended
Elman	57	RPROP/PSO	25	0.012	Ended
Elman	57	PSO	17	0.06	Ended
Elman	57	SA	127	0.045	Ended
Elman	5-75	RPROP, IP	10 epochs per node	0.0125	57 hidden nodes selected as best
Elman	57	RPROP	200	0.01	Ended
RBF	49	RPROP	418	0.0115	Gaussian
RBF	81	RPROP	243	0.0078	Mex. Hat
RBF	196	RPROP	716	0.00616	Mex. Hat
RBF	196	SVD	1	0.0727	Stagnant
SVM	-	-	1	0.0065	Stagnant

TABLE II
Final MSE Using DNI, Adjacent Stations & DWT

Net Type	# of Hidden Nodes	Training Regime	Epoch	MSE	Notes
MLP	157	RPROP	2600	0.0043	AT, H, SR,DNI (WGEN)
MLP	157	RPROP	2540	0.0047	AT, H, SR, DNI (Hoogenboom)
MLP	157	RPROP	3104	0.0043	AT,H,SR,DNI (Yang)
MLP	207	RPROP	1932	0.0044	A,H,SR, AWS
MLP	207	RPROP	2500	0.0043	All, AWS,DNI (Iqbal)
MLP	207	RPROP	3600	0.0048	All, AWS, DNI (ESRA2)
MLP	207	RPROP	3510	0.0043	Same w/DWT (D2)
MLP	207	RPROP	255	0.0051	Same w/DWT (H2)

All trials shown in Tables I and II use air temperature, humidity, solar radiation and rainfall as their input fields unless otherwise specified. It is important to note that the trials represented in Tables I and II were the best results for their respective configurations; trials with less accurate results have not been shown. Trials involving a greedy strategy halted before the network could achieve a lower MSE, so this strategy was abandoned in subsequent trials. Simulated annealing and particle swarm optimization strategies were relatively slow to train the networks they were used upon and would often halt before the network had completed training. The incremental pruning regime selected 57 hidden nodes as the configuration that produced the lowest MSE within a range of 5-75 hidden nodes. A larger range of hidden nodes was not tested, nor was incremental pruning implemented on a MLP. Moreover, the application of a support vector machine (SVM) showed promise by obtaining an MSE of 0.0065 after 1 epoch, but remained stagnant in subsequent epochs.

TABLE III
Final MSE for 1-Hr Predictions Using Varying Input Fields

Trial	A	B	C	D	E	F	G	H	I	J	K
Input Fields											
Day	x	x	x	x	x	x	x	x	x	x	x
Time	x	x	x	x	x	x	x	x	x	x	x
Air Temp.		x									
Humid.						x				x	
Dew Point					x						
Baro.Press.							x				
Wind Speed								x			
SR	x	x	x	x	x	x	x	x	x	x	x
TSR				x							x
PAR									x		x
Rainfall			x							x	
Prev. & Delta (4 hrs)											
Air Temp.		x									
Humid.						x				x	
Dew Point					x						
Baro. Press.							x				
Wind Speed								x			
SR	x	x	x	x	x	x	x	x	x	x	x
TSR				x							x
PAR									x		x
Rainfall			x							x	
Best MSE ($1x10^{-3}$)	4.3	4.3	4.4	4.5	4.5	4.5	4.6	4.8	5.7	4.4	5

Although the five models of DNI performed relatively the same, the WGEN consistently helped the prediction model attain a slightly lower MSE than the other models. Contrary to findings by [11], the addition of adjacent weather station SR data did not improve prediction accuracy. Likewise, preprocessing the SR data with a DWT did not improve prediction accuracy, and in some cases, hampered it. Trials where SR data were preprocessed with Coiflet and Legendre wavelet transforms are not shown, as the resulting MSE was not within an admissible range. Tables III and IV demonstrate the final MSEs obtained with various input parameters (e.g. rainfall, humidity, temperature, etc).

TABLE IV
FINAL MSE FOR 1-HR PREDICTIONS USING VARYING INPUT FIELDS

Trial	L	M	N	O	P	Q	R	S	T	U	V
Input Fields											
Day	x	x	x	x	x	x	x	x	x	x	x
Time	x	x	x	x	x	x	x	x	x	x	x
Air Temp.	x			x			x		x		x
Humid.	x		x		x	x	x		x		x
Dew Point											x
Baro.Press.							x				x
Wind Speed								x			x
SR	x	x	x	x	x	x	x	x	x	x	x
TSR		x		x	x	x		x	x	x	x
PAR		x	x	x	x			x		x	x
Rainfall	x	x	x			x	x	x	x	x	x
Prev. & Delta (4 hrs)											
Air Temp.	x			x			x		x		x
Humid.	x		x		x	x	x		x	x	x
Dew Point											x
Baro. Press.							x				x
Wind Speed								x			x
SR	x	x	x	x	x	x	x	x	x	x	x
TSR		x		x	x	x		x	x	x	x
PAR		x	x	x	x			x		x	x
Rainfall	x	x	x			x	x	x	x	x	x
Best MSE (1x10-3)	4.2	4.9	5	5.2	5.4	6	4.3	4.5	6.2	4.2	4.6

V. CONCLUSION

The results of the trials summarized in Tables I-IV suggest that the current air temperature, humidity, and solar radiation are the most vital inputs for accurately predicting solar radiation an hour into the future. This finding is intuitive, as the amount of water molecules suspended in the air influences the solar radiation that makes contact with the surface of the earth, and air temperature is an indication of the amount of solar radiation that has done so. Rainfall and DNI also serve as accurate predictors of solar radiation, though using both of these fields in combination did not appear to improve accuracy any more than using either field in isolation.

The MLP network with 157+ hidden nodes consistently yielded the most accurate predictions, despite other studies which have had success with recurrent networks [23], RBFNs [24], and SVMs [25], [26]. Likewise, the resilient propagation algorithm produced the most accurate predictions across trials, in comparison to the other training strategies implemented. Despite the success of this network configuration and training regime in regularly attaining an MSE below 0.0044, the addition of modeled DNI, adjacent weather station data, and preprocessing with DWT did not improve prediction accuracy, despite success demonstrated with these techniques within the time series literature [12], [8], [10], [27]. These findings suggest that either an MSE of 0.0042 is the limit for the most accuracy that can be attained with this particular data set, or that a (radically) different approach must be used for predicting hourly solar radiation.

Despite the breadth and diversity of the network configurations, input fields, and training strategies used in this study, there are still a number of approaches that may be taken in the future in an attempt to improve prediction accuracy. For one, other measures of error such as mean absolute error (MAE) and mean absolute percentage error (MAPE) may be used to determine whether models with similar MSE differ on these measures. Second, an autoregressive integrated moving average (ARIMA) and artificial neural network hybrid model may be implemented, as such models demonstrated accurate predictions in a number of other time series prediction problems [29], such as the British pound/US dollar exchange rate [28], sunspot appearance [31], and water quality [30], Third, the equations used to calculate the modeled DNI value could be adjusted to better fit solar radiation prediction. Fourth, the current model could be tested with data from other weather stations, in order to determine how its predictions generalize to other geographic regions. In conclusion, although the accuracy of the model was not improved beyond an MSE of 0.0042, the model remains more accurate than most models of solar radiation currently found within the literature.

REFERENCES

[1] Bodri, B. (2001). A neural-network model for earthquake occurrence. *Journal of Geodynamics*, 32(3), 289-310.
[2] *Ball, R. A., Purcell, L. C., & Carey, S. K. (2004)*. Evaluation of solar radiation prediction models in North America. *Agronomy Journal,* 96(2), 391-397.
[3] Thornton, P. E., Hasenauer, H., & White, M. A. (2000). Simultaneous estimation of daily solar radiation and humidity from observed temperature and precipitation: an application over complex terrain in Austria. *Agricultural and Forest Meteorology*, 104(4), 255-271.
[4] Mellit, A., &Pavan, A. M. (2010). A 24-h forecast of solar irradiance using artificial neural network: Application for performance prediction of a grid-connected PV plant at Trieste, Italy. *Solar Energy*, 84(5), 807-821.
[5] Elizondo, D., Hoogenboom, G., & McClendon, R. W. (1994). Development of a neural network model to predict daily solar radiation. *Agricultural and Forest Meteorology*, 71(1), 115-132.
[6] Rehman, S., &Mohandes, M. (2008). Artificial neural network estimation of global solar radiation using air temperature and relative humidity. *Energy Policy*, 36(2), 571-576.
[7] Hornik, K., Stinchcombe, M., & White, H. (1989). Multilayer feedforward networks are universal approximators. *Neural networks*, 2(5), 359-366.
[8] Gueymard, C. A. (2003). Direct solar transmittance and irradiance predictions with broadband models. Part I: detailed theoretical performance assessment. *Solar Energy*, 74(5), 355-379.
[9] Akansu, A. N., & Smith, M. J. (Eds.). (1996). Subband and wavelet transforms: design and applications (No. 340). *Springer*.
[10] Jensen, A., & la Cour-Harbo, A. (2001). Ripples in mathematics: the discrete wavelet transform. *Springer*.

[11] Li, B., McClendon, R. W., & Hoogenboom, G. (2004). Spatial interpolation of weather variables for single locations using artificial neural networks. *Transactions of the ASAE*, 47(2), 629-637.
[12] Richardson, C.W. & Wright, D.A. (1984). WGEN: A model for generating daily weather variables. U.S. Department of Agriculture, Agricultural Research Service, *ARS-8*, 83.
[13] Hoogenboom, G., Jones, J. W., Wilkens, P. W., Batchelor, W. D., Bowen, W. T., Hunt, L. A., ... & White, J. W. (1994). Crop models. *DSSAT* version, 3(2), 95-244.
[14] Yang, K., Huang, G. W., &Tamai, N. (2001). A hybrid model for estimating global solar radiation. *Solar energy*, 70(1), 13-22.
[15] Wong, L. T., & Chow, W. K. (2001). Solar radiation model. *Applied Energy*, 69(3), 191-224.
[16] Geiger, M., Diabaté, L., Ménard, L., & Wald, L. (2002). A web service for controlling the quality of measurements of global solar irradiation. *Solar energy*, 73(6), 475-480.
[17] Rigollier, C., Bauer, O., & Wald, L. (2000). On the clear sky model of the ESRA—European Solar Radiation Atlas—with respect to the Heliosat method. *Solar energy*, 68(1), 33-48.
[18] Badescu, V., Gueymard, C. A., Cheval, S., Oprea, C., Baciu, M., Dumitrescu, A., & Rada, C. (2012). Computing global and diffuse solar hourly irradiation on clear sky. Review and testing of 54 models. *Renewable and Sustainable Energy Reviews*, 16(3), 1636-1656.
[19] Paoli, C., Voyant, C., Muselli, M., &Nivet, M. L. (2010). Forecasting of preprocessed daily solar radiation time series using neural networks. *Solar Energy*, 84(12), 2146-2160.
[20] Igel, C. &Hüsken, M. (2000) Improving the Rprop Learning Algorithm. *Second International Symposium on Neural Computation* (NC 2000), 115-121.
[21] Igel,C. &Hüsken, M. (2003) Empirical Evaluation of the Improved Rprop Learning Algorithm. *Neurocomputing* 50:105-123.
[22] Connor, J. T., Martin, R. D., & Atlas, L. E. (1994). Recurrent neural networks and robust time series prediction. *Neural Networks, IEEE Transactions on*, 5(2), 240-254.
[23] Giles, C. L., Lawrence, S., &Tsoi, A. C. (2001). Noisy time series prediction using recurrent neural networks and grammatical inference. *Machine learning*, 44(1-2), 161-183.
[24] Cheng, E. S., Chen, S., &Mulgrew, B. (1996). Gradient radial basis function networks for nonlinear and nonstationary time series prediction. *Neural Networks, IEEE Transactions on*, 7(1), 190-194.
[25] Kim, K. J. (2003). Financial time series forecasting using support vector machines. *Neurocomputing*, 55(1), 307-319.
[26] Thissen, U., Van Brakel, R., De Weijer, A. P., Melssen, W. J., &Buydens, L. M. C. (2003). Using support vector machines for time series prediction. *Chemometrics and intelligent laboratory systems*, 69(1), 35-49.
[27] Grant, R. H., Hollinger, S. E., Hubbard, K. G., Hoogenboom, G., &Vanderlip, R. L. (2004). Ability to predict daily solar radiation values from interpolated climate records for use in crop simulation models. *Agricultural and forest meteorology*, 127(1), 65-75.
[28] Zhang, G. P. (2003). Time series forecasting using a hybrid ARIMA and neural network model. *Neurocomputing*, 50, 159-175.
[29] Ho, S. L., Xie, M., & Goh, T. N. (2002). A comparative study of neural network and Box-Jenkins ARIMA modeling in time series prediction. *Computers & Industrial Engineering*, 42(2), 371-375.
[30] ÖmerFaruk, D. (2010). A hybrid neural network and ARIMA model for water quality time series prediction. *Engineering Applications of Artificial Intelligence*, 23(4), 586-594.
[31] Khashei, M., &Bijari, M. (2011). A novel hybridization of artificial neural networks and ARIMA models for time series forecasting. *Applied Soft Computing*, 11(2), 2664-2675.